

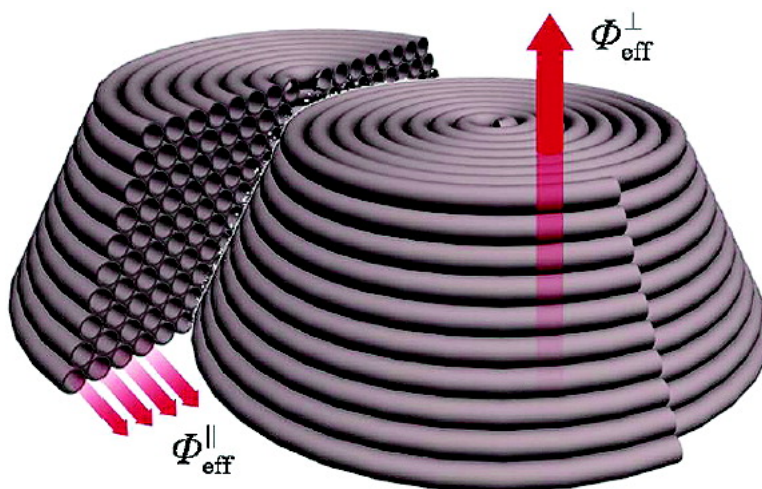
Article

Diffusion in Coiled Pores – Learning from Microrelease and Microsurgery

Magdalena Stempniewicz, Ahmed S. G. Khalil, Michael Rohwerder, and Frank Marlow

J. Am. Chem. Soc., **2007**, 129 (34), 10561-10566 • DOI: 10.1021/ja0728167 • Publication Date (Web): 08 August 2007

Downloaded from <http://pubs.acs.org> on February 15, 2009



More About This Article

Additional resources and features associated with this article are available within the HTML version:

- Supporting Information
- Links to the 3 articles that cite this article, as of the time of this article download
- Access to high resolution figures
- Links to articles and content related to this article
- Copyright permission to reproduce figures and/or text from this article

[View the Full Text HTML](#)



ACS Publications
 High quality. High impact.

Diffusion in Coiled Pores – Learning from Microrelease and Microsurgery

Magdalena Stempniewicz,^{†,‡} Ahmed S. G. Khalil,[†] Michael Rohwerder,[‡] and Frank Marlow^{*,†}

Contribution from the Max-Planck-Institut für Kohlenforschung, Kaiser-Wilhelm-Platz 1, 45470 Mülheim an der Ruhr, Germany, and Max-Planck-Institut für Eisenforschung, Max-Planck-Strasse 1, 40237 Düsseldorf, Germany

Received April 30, 2007; E-mail: marlow@mpi-muelheim.mpg.de

Abstract: The anisotropic diffusion in coiled pore systems of SBA-3-type microparticles has been studied by the release of guest molecules. The diffusion turns out as an example of the influence of hierarchical structuring on physical properties. Two modes of diffusion, associated with transport along and across the mesopores, can be identified and measured using optical microscopy. Redistribution between the two modes has been achieved by mesopore opening using two methods of “microsurgery”—either focused ion beams (FIB) or mechanical tools. The particles trimmed by FIB have revealed risks of misinterpretation of sample preparation with this tool. Instead of pure pore opening, the cutting by FIB resulted in simultaneous sealing of the mesopores.

1. Introduction

The continuing interest in hierarchical mesostructures, considering only recent studies,^{1–3} poses questions toward their particular properties that would eventually lead to special applications. By a hierarchical structure it is generally understood that different length scales need to be considered in order to characterize the structure. Mesoporous materials can be regarded hierarchical due to the different dimensions and ordering of the porosities. Because most applications of such materials make them serve as hosts, e.g., in catalysis or drug release, one of the most important properties is the diffusion characteristic. Diffusion is inherent to many transport processes so essential for successful preparation and functionality.

The “global” transport in a hierarchically organized mesostructure is a product of various complicated paths the guest molecules undertake in their journey through the different pores. Furthermore, the global effective diffusion coefficient of such a structure can be markedly influenced by the way the different levels of hierarchy are related to each other.³ There are, however, no literature data referring explicitly to the diffusion coefficients at a specific level of hierarchy. The problem of diffusion anisotropy in mesoporous materials has been addressed,⁴ but it has up-to-now not been regarded as an aspect of hierarchical structuring.

Silica mesostructures with coiled pores,³ such as fiber and conelike particles delivered by the SBA-3-type synthesis,^{5,6} are examples of hierarchies with complicated diffusion phenomena. The release of guest molecules encapsulated in coiled pores is typically determined by cross-wall transport (Figure 1A).⁷ It means that in order to find the way out from a particle the molecules have to force through the micropores connecting the mesopores. Since the flux is perpendicular to the silica walls, the diffusion coefficient associated with cross-wall transport is depicted by D_{eff}^{\perp} . At the same time, the transport along the mesopores, characterized by $D_{\text{eff}}^{\parallel}$, is not forbidden and occurs simultaneously.⁸ However, especially for the case of long fibers, the pore coiling and the perpendicularly applied concentration gradient favor the cross-wall transport hindering determination of the parallel coefficient. A similar effect has been shown on USY zeolite, where micropores rather than the bigger mesopores are the rate-determining factor.⁹

Here, we report on the determination of the parallel diffusion coefficient, $D_{\text{eff}}^{\parallel}$, on the example of a special SBA-3-type structure with coiled pores, namely conelike particles. The access to $D_{\text{eff}}^{\parallel}$ can be rendered by exposing mesopores to a concentration gradient as depicted schematically in Figure 1B. To induce a release determined by $D_{\text{eff}}^{\parallel}$, it would be sufficient to cut the particle near the central axis. Two methods of halving a particle have been tested to realize this concept: mechanical damage

[†] Max-Planck-Institut für Kohlenforschung.

[‡] Max-Planck-Institut für Eisenforschung.

- (1) Wang, J.; Xiao, Q.; Zhou, H.; Sun, P.; Yuan, Z.; Li, B.; Ding, D.; Shi, A.-C.; Chen, T. *Adv. Mater.* **2006**, *18*, 3284–3288.
- (2) Fujita, S.; Nakano, H.; Ishii, M.; Nakamura, H.; Inagaki, S. *Microporous Mesoporous Mater.* **2006**, *96*, 205–209.
- (3) Marlow, F.; Khalil, A. S. G.; Stempniewicz, M. *J. Mater. Chem.* **2007**, *17*, 2168–2182.
- (4) Stallmach, F.; Kärger, J.; Krause, C.; Jeschke, M.; Oberhagemann, U. *J. Am. Chem. Soc.* **2000**, *122*, 9237–9242.

- (5) Huo, Q.; Margolese, D. I.; Ciesla, U.; Feng, P.; Gier, T. E.; Sieger, P.; Leon, R.; Petroff, P. M.; Schüth, F.; Stucky, G. D. *Nature* **1994**, *368*, 317.
- (6) Huo, Q.; Margolese, D. I.; Stucky, G. D. *Chem. Mater.* **1996**, *8*, 1147–1160.
- (7) Stempniewicz, M.; Rohwerder, M.; Marlow, F. *ChemPhysChem* **2007**, *8*, 188–194.
- (8) KIRSTEIN, J.; PLATSCHKE, B.; JUNG, C.; BROWN, R.; BEIN, T.; BRÄUCHLE, C. *Nat. Mater.* **2007**, *6*, 303–310.
- (9) Kortunov, P.; Vasenkov, S.; Kärger, J.; Valiullin, R.; Gottschalk, P.; Elia, M. F.; Perez, M.; Stocker, M.; Drescher, B.; McElhiney, G.; Berger, C.; Glaser, R.; Weitkamp, J. *J. Am. Chem. Soc.* **2005**, *127*, 13055–13059.

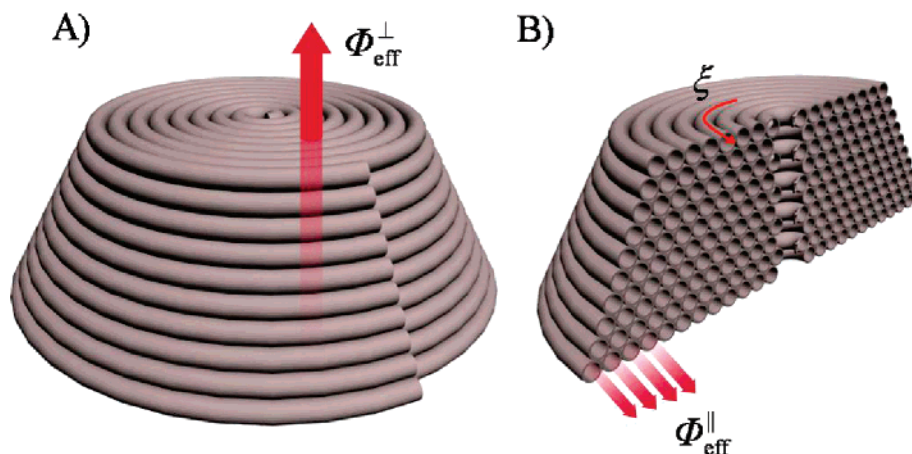


Figure 1. (A) Schematic structure of a conelike particle produced in an SBA-3-like synthesis. Release from a whole particle is determined by cross-wall transport connected with the flux $\Phi_{\text{eff}}^{\perp}$ and the effective diffusion coefficient D_{eff}^{\perp} . (B) After cutting a particle in half, diffusion along the pores becomes effective (flux $\Phi_{\text{eff}}^{\parallel}$ associated with $D_{\text{eff}}^{\parallel}$) with diffusion paths along ξ .

and trimming by the focused ion beam technique (FIB). Because of the desired, more-or-less localized nature of the damage the two methods will be called microdamage or microsurgery. The fact that the conelike particles can be grown on a flat support greatly facilitates such a manipulation of the sample. This is also of special importance for the measurement of release, which is conducted using optical microscope.

Besides the diffusion data, the release experiments provide information on the possible surface modification. Our results indicate that especially cutting with FIB causes sealing of external pore openings.

2. Experimental Section

2.1. Preparation of Conelike Particles. Mesoporous conelike particles on a glass support were prepared using SBA-3-type synthesis described elsewhere.¹⁰ The composition of the initial aqueous phase was (in moles) 100 H₂O:0.0246 CTAB:2.92 HCl:0.00022 Rh6G and 0.26 mmol of TBOS was used as a silica source. The cationic dye, Rhodamine 6G, served as a model guest molecule and was incorporated into the particles during the synthesis. The glass surface was modified using microcontact printing in order to enable the growth of conelike particles of well-defined lateral ordering. The ordering is not essential for the release measurement, but it simplifies sample manipulation, especially the addressing and finding of individual particles. The particles were used without further temperature treatment. After measurement of release, some of the samples were reloaded with dye by immersion in an aqueous solution of rhodamine for 3 h, completed by drying for 2 h at 50 °C.

The geometry of the particles, radius, and thickness were determined from optical microscopy using low depth-of-focus. For some samples the values were additionally confirmed by SEM.

2.2. Characterization of Release. Diffusion data are obtained from the kinetics of dye released from a single particle. The amount of dye is monitored by an optical microscope (Leitz, Orthoplan) with an attached camera (Ulead Eyepiece, 640 × 480 pixel). To diminish the influence of release from particles not being measured, the excess particles are removed from the glass support. On the selected area, a release cell is constructed using a spacer and a cover glass. The release experiment starts with the addition of water which is immediately sucked into the void between the support and the cover glass. Digital photographs are collected at appropriate time intervals until no more

loss of dye is observed. Further image analysis delivers absorption due to dye on the selected area, i.e., inside the particle. The CCD image is first decomposed in RGB (red, green, blue) channels. Because rhodamine is a red dye its absorption is mostly relevant in the green channel, which is used for further processing. The absorption extinction of an arbitrary point is obtained from

$$E(x) = -\log_{10} \frac{I(x) - I_0}{I_{100\%} - I_0} \quad (1)$$

where $I(x)$, $I_{100\%}$, and I_0 are the intensity at the position x at the sample, the reference intensity of 100% (no sample), and the dark current correction (black sample), respectively. To diminish the noise it is reasonable to consider an averaged $E(x)$ inside a particle, which corresponds to the mean concentration of dye in the selected measured area. A release curve is constructed by plotting the obtained absorption extinction against time. Diffusion data are obtained by fitting an appropriate release model to these data.

2.3. Microsurgery. Microsurgery of mesoporous particles refers to controlled damage induced either by physical machining using a fine razor blade or by localized sputtering with the focused ion beam (FIB). In each case the desired result is halving a conelike particle with a cut near the central axis. The FIB sputtering was performed in a Zeiss 1540 XB using Gallium ion gun operated at 30 keV. The time needed to trim a single particle varied with the applied gun current between 1 min (at 500 pA) and 2 h (at 5 pA).

3. Results

3.1. Release from Completely Intact Conelike Particles. Release from a parent conelike particle appears as a homogeneous loss of dye with no evident radial gradient under the microscope (Figure 3A). The time scale of the process already gives an idea of the dimension of the diffusion coefficient. We describe this time scale by the release time, $t_{1/2}$, which is the time at which the dye content drops by half. The typical value for whole parent particles is $t_{1/2} \approx 10$ min.

3.2. Microsurgery of Conelike Particles. The objective of microsurgery is to enable the release associated with transport along the mesopores by opening the mesopores. Because the mesopores are coiled around the central axis, the so-called singularity,¹¹ it is sufficient to make a cut in a plane near to

(10) Khalil, A. S. G.; Konjhdzic, D.; Marlow, F. *Adv. Mater.* **2006**, *126*, 1055–1058.

(11) Marlow, F.; Leike, I.; Weidenthaler, C.; Lehmann, C. W.; Wilczok, U. *Adv. Mater.* **2001**, *13*, 307–310.

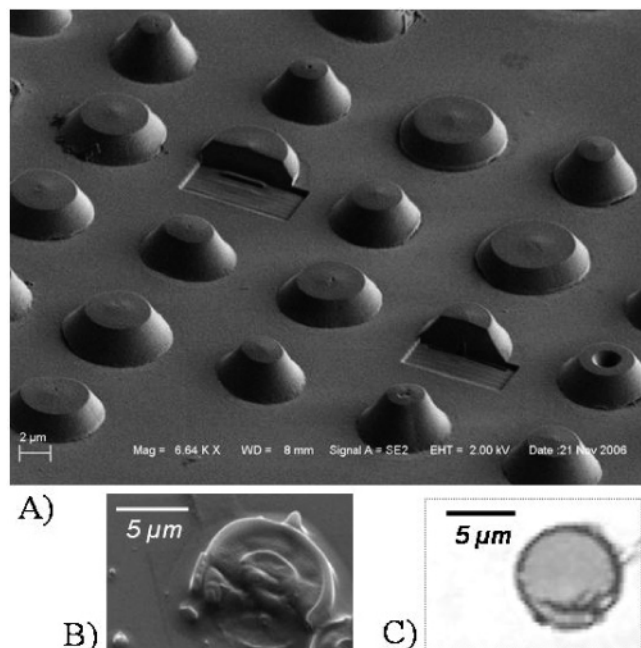


Figure 2. Microsurgery of conelike particles: (A) SEM of particles trimmed by focus ion beam (FIB); (B) SEM of mechanically damaged particle after secondary release; (C) Partially damaged particle (mechanical damage) seen in an optical microscope.

this axis. Such a high cut precision is only possible using an advanced technique like FIB.¹² The particles are visible with SEM during the operation (FIB), and the process is well controlled. A typical example is shown in Figure 2A. However, there is no guarantee that the silica matrix at the so-exposed surface will preserve its native structure. The high-energy Ga ions may induce changes.

Differently, in case of mechanical damage, there are not many reasons to expect structural changes. The unwanted part of a particle is smashed and swiped away without relevant interaction between the razor blade and the remaining part of the particle. However, the low precision and lack of controllability in the application of mechanical damage result typically in an irregular, ragged surface that does not necessarily contain the central axis (Figure 2B).

3.3. Observation of Modification Effects on Release. As in the whole parent particles, homogeneous loss of dye is observed in the FIB-trimmed particles. The rate of the dye loss is practically the same as that for a parent, nontrimmed particle measured in the same experiment (Figure 3A and C). The mechanically trimmed particles, in turn, lose their dye within tens of seconds as compared with tens of minutes in the case of whole particles. Ringwise emptying has been observed on partially damaged particles. The example in Figure 2B shows a notched particle that is initially uniformly filled with the dye. Upon release, the external rings are emptied within tens of seconds, whereas the inner part releases at a rate typical for an intact particle (Figure 3B).

3.4. Release Curves. Examples of release curves for a parent and for microdamaged particles are presented in Figure 4. The deduced release times confirm the visually fast release in the case of mechanical damage and the similar time scale in the

case of FIB-trimming. It is worth noting that this observation is independent from the interpretation below (section 4.2).

3.5. Secondary Release. After completing the release measurement (primary release) some of the particles were subject to the aqueous rhodamine solution to refill the pores. After drying, release was measured once more (secondary release). The characteristic difference in release times between a parent and a mechanically damaged particle observed in primary release is decrease in the secondary process. The release time of the whole particle changes from $t_{1/2} = 12$ min to 16 min. The same change of the damaged particle is from $t_{1/2} = 2$ min to 15 min. The principal behavior of the release curves (not shown) is unchanged.

4. Discussion

4.1. Two Diffusion Processes. The coiled pore structure of conelike particles is very similar to that of SBA-3-like fibers.¹⁰ On this basis, it can be concluded that release from the conelike particles will analogously be determined by cross-wall transport.⁷ The kinetics of such release are characterized by the same effective diffusion coefficient D_{eff}^{\perp} . Diffusion parallel to the coiled pores is possible at any time; however, it does not affect the release kinetics. It can only become the rate-determining factor when the mesopores are opened in such a way that the molecule's path along the pore is comparable with the lateral dimension of the releasing particle. The release will then mainly be characterized by the effective diffusion coefficient $D_{\text{eff}}^{\parallel}$. $D_{\text{eff}}^{\parallel}$ is expected to be much larger than D_{eff}^{\perp} because the perpendicular coefficient involves transport through the intrawall pores. The size of these pores is likely comparable with the size of guest molecules resulting in a confinement of the space in which molecules can move. In zeolites, such an effect is known to result in lowering the diffusion coefficient.^{13,14}

The clearly faster emptying of mesopores observed in the mechanically damaged particles confirms obviously the relation between the coefficients. Especially the ringwise emptying of partially damaged particles (Figure 3B) speaks for the considerably faster transport along the mesopores.

4.2. Determination of D_{eff}^{\perp} and $D_{\text{eff}}^{\parallel}$. The quantification of the diffusion coefficients requires the application of a release model. Such a model is strongly dependent on the assumed geometry of release, and its choice is essential for the numerical results.¹⁵ In the case of regular particles, spheres, or fibers, the geometry is fully symmetric—spherical or cylindrical. A wholly intact conelike particle, however, represents a complex geometry since transport proceeds in both axial and radial directions. The proper model should be a combination of plane-sheet and cylinder geometries. However, the flatter the particle, the more relevant the plane-sheet geometry becomes. Because most of the measured particles are rather flatter than broader ($L < R$), the plane-sheet geometry is favored.

The absorption values in the microscopic data are proportional to the mean concentration of dye present in a particle at a given time. A release model can be therefore derived by calculation of the mean concentration from the concentration profile known

(12) Sugiyama, M.; Sigesato, G. *J. Electron Microsc.* **2004**, *53*, 527–536.

(13) Kärger, J.; Petzold, M.; Pfeifer, H.; Ernst, S.; Weitkamp, J. *J. Catal.* **1992**, *136*, 283.

(14) Kärger, J.; Stallmach, F.; Vasenkov, S. *Magn. Reson. Imaging* **2003**, *21*, 185–191.

(15) Marlow, F.; Stempniewicz, M. *J. Phys. Chem. B* **2006**, *110*, 11604–11605.

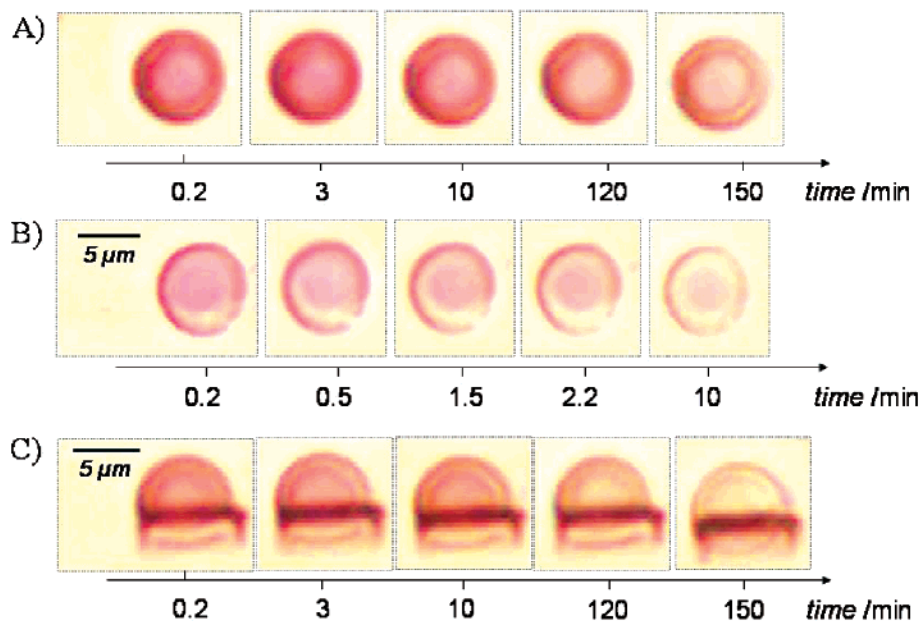


Figure 3. Release observed with optical microscope from (A) a whole parent particle, (B) the partially damaged particle shown in Figure 2C, and (C) a particle trimmed by FIB. Emptying of the mechanically opened pores, visible a ring in (B), proceeds much faster than emptying of both whole and FIB-trimmed particles.

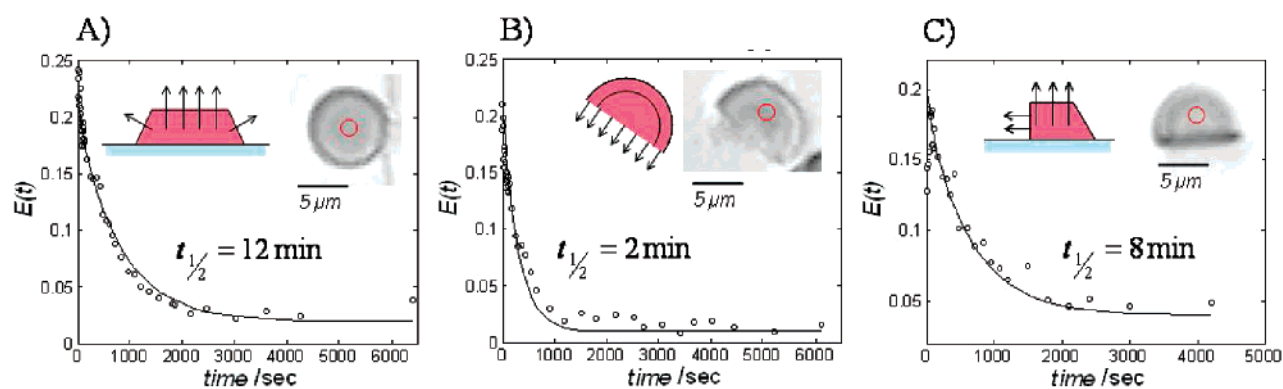


Figure 4. Measured loss of dye from (A) parent particle, (B) mechanically damaged particle, and (C) FIB-trimmed particle, with indicated release times. The included schemes represent the relevant probable release directions. The fitted release curves are explained in section 4.2. The particles in A and B were investigated in the same experiment (one series of photos).

from the solution of the diffusion equation in plane-sheet geometry.¹⁶ The time evolution of the mean concentration is

$\bar{c}(t) =$

$$c_{\text{const}} + c_{\text{init}} \frac{8}{\pi^2} \sum_{n=0}^{\infty} \frac{1}{(2n+1)^2} \exp\left(-\frac{D_{\text{eff}}^{\perp}(2n+1)^2\pi^2 t}{4L^2}\right) \quad (2)$$

where c_{init} and L are the initial concentration in the particle and the particle thickness, respectively. The constant c_{const} is introduced to compensate for the disturbing contributions (scattering and surface reflection) to the particle extinction and the fact that the volume of the up-taking solvent is limited. The limited volume does not satisfy the requirement of the perfect sink condition throughout the experiment and leads to a remnant amount of dye at equilibrium.

For comparative purposes a release function in the cylinder geometry can be derived, using the same argumentation as that of the literature.¹⁶

In the case of halved conelike particles the geometry of release is heavily changed. The molecules can take arclike paths along the coiled pores, ξ (see Figure 1 B), which leads to a complicated geometry. However, assuming the dominance of this transport, the flux is uniaxial along ξ and can be approximated by plane-sheet geometry with the mean characteristic length $\bar{\xi}$. In this simplification, cross-wall transport is fully neglected and the associated diffusion coefficient is only $D_{\text{eff}}^{\parallel}$. The characteristic length can be expressed by particle radius, $\bar{\xi} = \pi/4 R$. For a reasonably small area at which intensity is measured, the release function can be described by the concentration in a plane-sheet at $\xi = 0$:

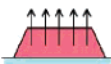
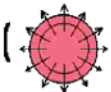

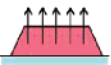
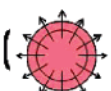
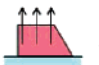

$c(t) =$

$$c_{\text{const}} + c_{\text{init}} \frac{4}{\pi} \sum_{n=0}^{\infty} \frac{(-1)^n}{2n+1} \exp\left(-\frac{D_{\text{eff}}^{\parallel}(2n+1)^2\pi^2 t}{4\bar{\xi}^2}\right) \quad (3)$$

Models (2) and (3) are very similar mathematically and both fit very well to each experimental set similar as in other release-and-uptake phenomena.¹⁵ However, they are associated with

(16) Crank, J. *The Mathematics of Diffusion*, 2nd ed.; Oxford Press: 1975; pp 47 and 73.

Table 1. Diffusion Coefficients Determined for Parent and Mechanically Damaged Particles from Both Primary and Secondary Releases^a

	whole particle	mechanically damaged
primary release	 $D_{\text{eff}}^{\perp} = 2.0 \cdot 10^{-11} \text{ cm}^2 \text{ s}^{-1}$  $D_{\text{eff}}^{\perp} = 1.8 \cdot 10^{-11} \text{ cm}^2 \text{ s}^{-1}$	 $D_{\text{eff}}^{\parallel} = 3.5 \cdot 10^{-10} \text{ cm}^2 \text{ s}^{-1}$
secondary release	 $D_{\text{eff}}^{\perp} = 7.9 \cdot 10^{-12} \text{ cm}^2 \text{ s}^{-1}$  $D_{\text{eff}}^{\perp} = 9.1 \cdot 10^{-12} \text{ cm}^2 \text{ s}^{-1}$	 $D_{\text{eff}}^{\perp} = 8.9 \cdot 10^{-12} \text{ cm}^2 \text{ s}^{-1}$  $D_{\text{eff}}^{\parallel} = 7.0 \cdot 10^{-11} \text{ cm}^2 \text{ s}^{-1}$

^a The geometry of the used model is indicated by an icon. The results in brackets are the disfavored option (see text). The apparent change of diffusion coefficient for the second release is ascribed to sealing of pore openings.

different diffusion coefficients and different characteristic lengths. It should be kept in mind that these two coefficients express different modes of diffusion. It implies that, in a mixed case, when both parallel and perpendicular transports are enabled, it is impossible to assign the fit number to either D_{eff}^{\perp} or $D_{\text{eff}}^{\parallel}$. Such mixing might occur when the mesopores at the cut surface are only partially opened.

Figure 4A and B show release curves obtained for a whole parent particle and a mechanically damaged one, measured in the same experiment. They have clearly different release times, and therefore, we assign them to the two different modes of release discussed above. Fitting with the models results in the parallel and perpendicular diffusivities which differ by an order of magnitude: $D_{\text{eff}}^{\perp} = 2.0 \times 10^{-11} \text{ cm}^2 \text{ s}^{-1}$ as compared with $D_{\text{eff}}^{\parallel} = 3.5 \times 10^{-10} \text{ cm}^2 \text{ s}^{-1}$. Noteworthy, the determined value of D_{eff}^{\perp} is comparable with the one corresponding to a SBA-3-like fiber, $D_{\text{eff}}^{\perp} = 3.7 \times 10^{-11} \text{ cm}^2 \text{ s}^{-1}$, obtained with the same microscopic method.

It should be kept in mind that the value of $D_{\text{eff}}^{\parallel}$ was derived assuming a fully irrelevant cross-wall transport and using a release function based on certain approximations. The former is justified by the large difference between the two diffusion coefficients and the fact that the concentration gradient driving both modes of release acts on a very similar length. The approximation in release functions include neglecting the surface diffusion barrier, which might result in lowering of the effective coefficients.

The obtained numbers are fully consistent with the qualitative observation of release. They clearly explain why the release from mechanically damaged particles is accelerated so much.

4.3. Modification of the Particles. The modified release from particles exposed to microdamage can provide indications of an external surface diffusion barrier and sealing of the pore openings. Release from the FIB-trimmed particles shows no changed release constant, which strongly indicates pore sealing at the trimmed surface. Such a sealing effect is known, and

desired, in the case of plasma etching of silica.¹⁷ However, sealing of pores in the meso-range has not been reported so far.¹⁸ But unlike the case of plasma etching, there are no film forming molecules transferred in the case of FIB; therefore, the sealant must originate from the damaged and rearranged silica of the parent matrix. There are no data available in literature concerning damage to mesoporous silica induced by ion bombardment, but the lack of accelerated release from the FIB-trimmed particles we regard as a strong indication of such damage.

Another kind of sealing can be demonstrated on particles with surface modified intentionally by water treatment.⁷ The modified release was measured on particles reloaded with the dye after the primary release. The modification can be mainly associated with the surface barrier reported previously for SBA-3-like fibers.⁷ Such a surface barrier has two effects: (1) it changes the release especially at long release times and (2) it may change the main release path. Although the qualitative observation indicates the presence of a surface barrier, for modeling of the modified release, eqs 2 and 3 can be used particularly for short release times. The noise in data, especially at long release times, makes the fit very unstable when a surface diffusion barrier is allowed. The presence of the barrier might, however, be the result of a small apparent drop of the diffusion coefficient.

In the case of secondary release from the mechanically damaged particle we have observed release times very similar to those for parent particles and for FIB-modified particles. Therefore, we conclude that the former open pores have been closed again by the surface barrier and the model (3) is not applicable anymore.

The determined diffusion coefficients are collected in Table 1. The coefficients found for a whole parent particle drop by a factor of ~ 2.5 after modification. Whereas, the change for a mechanically damaged particle lies between 12 and 40 depend-

(17) Mannaert, G.; Baklanov, M. R.; Le, Q. T.; Travaly, Y.; Boullart, W.; Vanhaelemeersch, S.; Jonas, A. M. *J. Vac. Sci. Technol., B* **2005**, *23*, 2198–2202.

(18) van Bavel, M.; Beyer, G.; Abell, T.; Iacopi, F.; Shamiryan, D.; Maex, K. *Future Fab* **2003**, *16*, 111–114.

ing on the assumed model (Table 1). This difference shows how drastic sealing of the mesopores can be.

5. Conclusions

Structures with coiled pores offer a unique possibility for the study of diffusion in mesoporous materials. Using optical microscopy, the anisotropic 3D diffusion in the complex mesoporous structures has been visualized and quantified. The release is enabled by either cross-wall transport or diffusion along the mesopores.

The characteristic diffusion coefficients have been determined from the study of particles with induced microdamage. They differ by an order of magnitude; i.e., $D_{\text{eff}}^{\parallel}/D_{\text{eff}}^{\perp} \sim 10$ was found for the molecule Rh6G in as-made SBA-3-like structures. This ratio demonstrates how strongly diffusion can be varied in appropriately designed hierarchical structures of pores. It exemplifies how the properties of a hierarchical structure are principally affected by the anisotropy of a specific sublevel of the hierarchy.

The two techniques of the microsurgery, focused ion beam (FIB) and mechanical damage, used here for sample preparation,

provided some additionally interesting information. Interaction with ions during FIB-trimming leads to sealing of the mesopores at the cut surface. Likewise, immersion in water results in a blocking of the mesopore openings as well. These modifications are options but also can cause problems for the investigation of nanostructures. The effects induced by FIB, for instance, may render it unserviceable in the preparation of TEM samples of mesoporous systems. Especially, the pore openings, both the outermost intrawall connections and the openings of mesopores seem to be quite unstable. However, controlled modifications could be utilized for purposeful pore sealing, as it may be desired in electronic applications.¹⁸

Acknowledgment. The authors kindly acknowledge the International Max-Planck Research School for Surface and Interface Engineering in Advanced Materials (SurMat) for support. The authors would like to thank Dr. Stefan Zaeferrer and Mrs. Monika Nellessen for the valuable and extensive help with FIB.

JA0728167